Strain-assisted spin manipulating and the discerption of strain-induced spin splitting

Yuan Li and You-Quan Li
Zhejiang Institute of Modern Physics and Department of Physics, Zhejiang University, Hangzhou 310027, P. R. China
(Received February 2, 2008)

We show that the efficiency of manipulating electron spin in semiconductor quantum wells can be enhanced by tuning the strain strength. The effect combining intrinsic and strain-induced spin splitting varies for different systems, which provides an alternative route to understand the experimental phenomena brought in by the strain. The types of spin splittings caused by strain are suggested to be distinguished by the measurement of the electron-dipole-spin-resonance intensity through changing the direction of the *ac* electric field in the *x*-*y* plane of the quantum well and tuning the strain strengths.

PACS numbers: 71.70.Fk, 78.67.De, 71.70.Ej, 85.75.-d

I. INTRODUCTION

Manipulating electron spins by an external electric field is a central issue in the realization of spintronics on the basis of solid-state materials [1, 2, 3, 4] as it is important for quantum computing and information processing [5]. In the experiment by Kato et al. [6] electron spins are manipulated by means of the voltage-controlled g-tensor modulation technique which is applicable for materials with small g-tensor merely. Recently, a mechanism called electric dipole spin resonance (EDSR) was proposed to investigate spin manipulating for electrons in a parabolic quantum well [7, 8]. An in-plane or a perpendicular electric field was shown to efficiently manipulate the spin for electrons in quantum wells. In that mechanism a tilted magnetic field is required but small g-tensor is not necessary.

It has been recognized recently that a strain-induced spin splitting is able to effectively manipulate electron spins without magnetic fields, which provides an alternative route, called strain engineering, for solid-state spin manipulation. For example, it has been employed to control electron-spin precession [9, 10, 11] in zinc-blende structure semiconductors and to tune the spin coherence with a significant enhancement of the spin dephasing time [12]. In semiconductor epilayers, the effect of the strain on electron-spin transport [13] and that of uniaxial tensile strain on spin coherence [14, 15] have also been carried out in recent experiments. The types of strain-induced spin splittings in strained bulk semiconductors were analyzed [16] theoretically, whereas, it is not very clear so far that which type of spin splitting (i.e., Rashba-type or Dresselhuas-type) produced by the strain [9, 16] plays an important role in manipulating electron spins. Since the spin manipulating in terms of strain is easily realizable in practical devices, it will be useful to exhibit the type of strain-induced spin splitting.

In this paper, we show that the efficiency of spin manipulation for electrons can be enhanced through adjusting the strain strength of the semiconductor quantum wells. The effect combining intrinsic and strain-induced spin splitting varies for different systems. We propose a method to identify whether the spin splitting induced by strain is of Dresselhuas-type or Rashba-type. This paper is organized as follows: In next section, we give a general consideration on the electron-dipole spin resonance caused by both the intrinsic and strain-induced spin splitting. In Sec. III and Sec. IV, we consider the systems with intrinsic spin-orbit coupling of Dresselhaus type and Rashba-type respectively. The spin manipulation for an InSb quantum well imposed with strain is investigated by means of the orbital mechanism. As a comparison, the combining effects of intrinsic and strain-induced spin splitting in some other kind of semiconductor quantum wells are also studied. A summary of our main conclusion is given in the last section.

II. GENERAL CONSIDERATION

For electron gases in quantum wells or two-dimensional heterostructures of certain semiconductors, there exist two intrinsic spin-orbit couplings called Dresselhaus and Rashba couplings that arise from the bulk-inversion asymmetry or the structure-inversion asymmetry of the material, respectively. The Dresselhaus type spin-orbit interaction can be obtained by averaging the corresponding bulk expression over the motion relevant to the confined degree of freedom [17]. If the first electron subband is merely populated in [001] quantum wells with the growth direction along the z-axis, the Dresselhaus type Hamiltonian $H_{in}^{\rm D}$ is given by,

$$H_{in}^{\rm D} = \sigma_x k_x(\lambda k_y^2 - \beta) + \sigma_y k_y(\beta - \lambda k_x^2), \qquad (1)$$

where $\beta = \lambda\langle k_z^2\rangle$ with λ denoting the Dresselhaus spin-orbit coupling strength and $\langle k_z^2\rangle$ being averaged over the ground state. Here $H_{in}^{\rm D}$ contains both linear and cubic terms in k.

The Rashba spin-orbit interaction can be written as [18, 19],

$$H_{in}^{\rm R} = \alpha(\sigma_x k_y - \sigma_y k_x), \qquad (2)$$

where α refers to the Rashba spin-orbit coupling strength. In some systems, the Rashba or the Dressel-

haus spin-orbit coupling dominates over the other effects. In order to manipulate electron spins efficiently, it becomes important to know the relative strengths between Rashba and Dresselhaus interactions in the system under consideration.

In zinc-blende type semiconductors, strain introduces additional spin splitting which can be of structure-inversion-asymmetry type [20],

$$H_{st}^{\rm R} = \frac{1}{2}C_3[\sigma_x(\epsilon_{xy}k_y-\epsilon_{xz}k_z)+\sigma_y(\epsilon_{yz}k_z-\epsilon_{yx}k_x) +\sigma_z(\epsilon_{zx}k_x-\epsilon_{zy}k_y)]. \quad (3)$$

It can also be of bulk-inversion-asymmetry type if the diagonal elements ϵ_{ij} are included

$$H_{st}^{\rm D} = D[\sigma_x k_x(\epsilon_{zz}-\epsilon_{yy})+\sigma_y k_y(\epsilon_{xx}-\epsilon_{zz}) +\sigma_z k_z(\epsilon_{yy}-\epsilon_{xx})]. \quad (4)$$

Here C_3 and $D > 0$ are material constants, and ϵ_{ij} $(i,j=x,y,z)$ denotes the symmetric strain tensor. We call $H_{in}^{\rm D}$ and $H_{in}^{\rm R}$ in Eqs. (1) and (2) intrinsic spin-orbit couplings so as to distinguish them from the strain-induced spin splittings in Eqs.(3) and (4). These four types of spin-orbit interactions may take place simultaneously if strain is exerted on a sample. However, they can play different roles in manipulating electron spins. It is worthwhile to study which kind of strain-induced spin splittings plays an important role in spin manipulation in various semiconductor quantum wells.

In order to carry out a general calculation of electron-dipole-spin-resonance intensity for semiconductor quantum wells with spin-orbit interactions, we consider

$$H = H_0 + H_{so} + e\mathbf{E}(t)\cdot\mathbf{r}, \quad (5)$$

which describes two-dimensional electrons with spin-orbit coupling in a parabolic quantum well. An in-plane *ac* electric field $\mathbf{E}(t) = E(t)(\cos\phi, \sin\phi, 0)$ and a tilted magnetic field $\mathbf{B}(\theta,\varphi)$ with θ and φ being the polar and azimuthal angle of B together with a strain are applied to the system. Accordingly, the first part in Eq. (5) reads

$$H_0 = \frac{1}{2m^\star}(\mathbf{p}+\frac{e}{c}\mathbf{A})^2 + \frac{1}{2}m^\star\omega_0^2 z^2 + \frac{g}{2}\mu_B\sigma\cdot\mathbf{B},$$

where $\mathbf{A}$ is the vector potential of the tilted magnetic field, $m^\star$ denotes the effective mass of the electron, and ω_0 characterizes the parabolic potential well. The second part H_{so} in Eq. (5) may include either intrinsic or strain-induced spin-orbit couplings.

To diagonalize the Hamiltonian H_0, one needs to rotate the original coordinate frame $\{\hat{x},\hat{y},\hat{z}\}$ to the new one $\{\hat{x}',\hat{y}',\hat{z}'\}$, where $\hat{z}'$ is chosen in alignment with the orientation of $\mathbf{B}$, $\hat{y}'$ is lying in x-y plane, and $\hat{x}'$ is chosen to form a right-hand triple with $\hat{y}'$ and $\hat{z}'$. Thus the coordinates in both frame systems are related, $(\hat{x},\hat{y},\hat{z}) = (\hat{x}',\hat{y}',\hat{z}')R^T$, by

$$R = \begin{pmatrix} \cos\theta\cos\varphi, & -\sin\varphi, & \sin\theta\cos\varphi \\ \cos\theta\sin\varphi, & \cos\varphi, & \sin\theta\sin\varphi \\ -\sin\theta, & 0, & \cos\theta \end{pmatrix},$$

which also relates the momentum components in the two frame systems, $k_i = R_{ij}k_j'$ (here $i,j=x,y,z$). By using the Landau gauge $\mathbf{A} = (0, Bx', 0)$, H_0 can be written as the sum of two harmonic oscillators [8] and its energy levels are given by,

$$E_s(n_+,n_-) = \hbar\omega_+\big(n_+ + \frac{1}{2}\big) + \hbar\omega_-\big(n_- + \frac{1}{2}\big) + \frac{s}{2}\hbar\omega_z, \quad (6)$$

where $s = \pm 1$ label the spin states and $n_\pm$ refer to the orbital quantum numbers, $\omega_\pm(\theta)$ are the frequencies of the coupled cyclotron-confinement modes

$$\omega_\pm^2(\theta) = \frac{\omega_0^2+\omega_c^2 \pm \Delta^2\ \mathrm{sgn}(\omega_0-\omega_c)}{2},$$
$$\Delta^2 = (\omega_0^4+\omega_c^4-2\omega_0^2\omega_c^2\cos 2\theta)^{1/2}. \quad (7)$$

If the spin-orbit coupling H_{so} is relatively small in comparison to other energy scales, such as the confinement energy $\hbar\omega_0$, the cyclotron energy $\hbar\omega_c = \hbar eB/m^\star c$ and Zeeman-splitting energy $\hbar\omega_z = g\mu_B B$, one can calculate the EDSR intensity by employing the method proposed in Ref. [8]. The strategy of this method is to eliminate the terms related to spin-orbit couplings in the original Hamiltonian with the help of a canonical transformation e^F. After some algebraic calculations, the operators of coordinates and momenta in original coordinate can be expressed as linear combinations of the creation and annihilation operators of the harmonic oscillators. Furthermore, the spin-orbit coupling H_{so} and the interaction term $e\mathbf{E}(t)\cdot\mathbf{r}$ can be expressed in terms of the creation and annihilation operators. The EDSR intensity $I \propto \mid T \mid^2$ is obtained by evaluating the matrix T which characterizes the spin-flip transitions induced by the *ac* electric field $\mathbf{E}(t)$, namely,

$$T = \frac{1}{E(t)}\langle n_+,n_-,\uparrow\mid \mathbf{E}(t)\cdot\big[\hat{F},\,\mathbf{r}\big]\mid n_+,n_-,\downarrow\rangle. \quad (8)$$

Here the operator $\hat{F}$ is perturbatively determined by the following relation

$$\langle n_+',n_-',s'\mid\hat{F}\mid n_+,n_-,s\rangle = \frac{\langle n_+',n_-',s'\mid H_{so}\mid n_+,n_-,s\rangle}{E_{s'}(n_+',n_-') - E_s(n_+,n_-)} + \text{high order}. \quad (9)$$

This is the condition for the cancellation of the spin-orbit coupling term H_{so} with the first order (or further orders if necessary) perturbation terms brought in by the canonical transformation $e^{\hat{F}}$ which connects the eigenstates of H_0+H_{so} with the eigenstates of H_0. Note that the Pauli matrices as well as $\mathbf{r}$ appeared in Eq. (5) are with respect to the original coordinate frame $\{\hat{x},\hat{y},\hat{z}\}$. They should also be reexpressed with respect to the new coordinate frame $\{\hat{x}',\hat{y}',\hat{z}'\}$ so that Eqs. (8) and (9) are computable.

III. SYSTEMS WITH INTRINSIC DRESSELHAUS COUPLING

A. Strain-induced Rashba-type coupling

We firstly consider the strain-induced Rashba-type spin splitting for the systems with intrinsic Dresselhaus coupling (we call D+R case for brevity). An concrete example of such a system is an InSb quantum well [21], where $H_{in}^{\rm D}$ dominates over $H_{in}^{\rm R}$ with typical value $\lambda = 200\,{\rm eV\AA}^3$ [22]. The application of diagonal strain on the InSb quantum well in the $x, y, z = [100], [010], [001]$ directions does not introduce any observable spin splitting but the shear strain leads to a splitting described by $H_{st}^{\rm R}$ [16, 23]. For compression along the [110] axis, $\epsilon_{xy} = \epsilon'_{110}/2$ and the strain ϵ'_{110} is given by

$$\epsilon'_{110} = \epsilon_{110} - \epsilon_{1\bar{1}0} = \frac{1}{2} S_{44} P_{110},$$

where S_{44} and P_{110} are the compliance coefficient and the applied stress, respectively. Accordingly, $\epsilon_{xz}{=}\epsilon_{yz} = 0$ and the electric field is in-plane ($\langle\ k_z\ \rangle = 0$), then the spin precession for two dimensional electrons in the InSb quantum well under the above strain configuration is described by the following Hamiltonian

$$\begin{aligned} H_{so}^{\rm D+R} &= H_{in}^{\rm D} + H_{st}^{\rm R} \\ &= \beta(\sigma_y k_y - \sigma_x k_x) + \gamma(\sigma_x k_y - \sigma_y k_x) \\ &\quad +\lambda(\sigma_x k_x k_y^2 - \sigma_y k_y k_x^2), \end{aligned} \tag{10}$$

where the strain parameter $\gamma = \frac{1}{2} C_3 \epsilon_{xy}$, $C_3 = 1.13 \times 10^{-7}$eVcm [24, 25]. The former two terms in Eq. (10) are linear in momenta so that it appears as linear combination of the creation and annihilation operators. The last term is cubic in k for which we only need to keep those part with nonvanishing contribution to the matrix element of Eq. (8). As we kept the term proportional to λ in the original Hamiltonian, we have to account for the second order terms appearing after the canonical transformation. After tedious calculation, we find that the term proportional to $\gamma\beta$ vanishes while the term proportional to λ remains. As a result, in the lowest energy level, $n_+ = n_- = 0$, we obtain from the formula (8) that

$$\begin{aligned} T^{\rm D+R} = &-\frac{\lambda}{\hbar Q_3} \sum_{\nu=+,-} \Big\{ [\omega_c \cos(\varphi-\phi)\cos\theta + i\omega_z \sin(\varphi-\phi)]\Omega Q_\nu Q_1 \\ &+[\Omega\omega_c \cos\theta \sin(\varphi-\phi) - i\omega_z \cos(\varphi-\phi)(\Omega + \omega_c^2 \sin^2\theta)] Q_\nu Q_2 \Big\} + \frac{\beta}{\hbar Q_3} \Big\{ \cos(\varphi-\phi) \times \\ &[\Omega\omega_c \cos\theta (i\cos 2\varphi - \sin 2\varphi \cos\theta) + \omega_z(\Omega + \omega_c^2 \sin^2\theta)(\sin 2\varphi - i\cos 2\varphi \cos\theta)] \\ &+i\sin(\varphi-\phi)\Omega[\omega_z(i\cos 2\varphi - \sin 2\varphi\cos\theta) + \omega_c \cos\theta(\sin 2\varphi - i\cos 2\varphi\cos\theta)] \Big\} - \frac{\gamma}{\hbar Q_3} \Big\{ \\ &\cos(\varphi-\phi)[\Omega\omega_c \cos^2\theta + \omega_z(\Omega + \omega_c^2 \sin^2\theta)] + i\cos\theta \sin(\varphi-\phi)(\omega_c + \omega_z)\Omega \Big\}, \end{aligned} \tag{11}$$

where

$$\begin{aligned} Q_1 &= \Big(\frac{\cos\theta}{2} + i\cot 2\varphi\Big) Q_4 + (\cos\theta \sin 2\varphi - i\cos 2\varphi) \\ &\quad \times (1 - \frac{\omega_+^2}{\omega_c^2}) \frac{\omega_c^2}{\Delta^2}\ {\rm sgn}(\omega_0 - \omega_c), \\ Q_2 &= \frac{3}{2} i Q_4 + (\cos\theta \cos 2\varphi + i \sin 2\varphi) \\ &\quad \times (1 - \frac{\omega_+^2}{\omega_c^2}) \frac{\omega_c^2}{\Delta^2}\ {\rm sgn}(\omega_0 - \omega_c), \\ Q_3 &= \omega_0^2(\omega_c^2 \cos^2\theta - \omega_z^2) - \omega_z^2(\omega_c^2 - \omega_z^2), \\ Q_4 &= -\frac{\omega_c^2}{\Delta^2} \sin 2\varphi \sin^2\theta\ {\rm sgn}(\omega_0 - \omega_c), \\ Q_\pm &= m^\star \omega_\pm / 2\hbar \\ \Omega &= \omega_0^2 - \omega_z^2. \end{aligned}$$

The terms proportional to β and γ in Eq.(11) are in agreement with the results [8] for pure Dresselhaus and Rashba spin-orbit couplings. Then we are in the position to evaluate the EDSR intensity, $I \propto |\ T\ |^2$, numerically.

Firstly, we investigate the angular dependence of the EDSR intensity for the InSb based quantum well under strain. As illustrated in top panel of Fig. 1, the EDSR intensity will increase when the magnetic field is tilted. This feature implies that the manipulation of electron spins becomes more efficient once a tilted magnetic field is introduced. In our calculation, the system's parameters are chosen by referring to experimental situations, *i.e.*, $\lambda = 200\,{\rm eV\AA}^3$, $C_3 = 1.13 \times 10^{-7}$eVcm, $\omega_z/\omega_c = -0.32$, $\omega_0 = 2eB_0/(m^\star c)$ with $B_0 = 2\,{\rm T}$, $\beta = \lambda\langle\ k_z^2\ \rangle = \lambda m^\star \omega_0/(2\hbar)$ and $m^\star = 0.014 m_0$ with m_0 being the mass of free electron. We set $\beta = 1$ for convenience in numerical calculation. It is more important for us to observe the influence of the strain on the spin manipulating described by EDSR. The figure in the bottom panel of Fig. 1 shows that the strain-induced Rashba-type spin splitting makes the characteristic of the EDSR

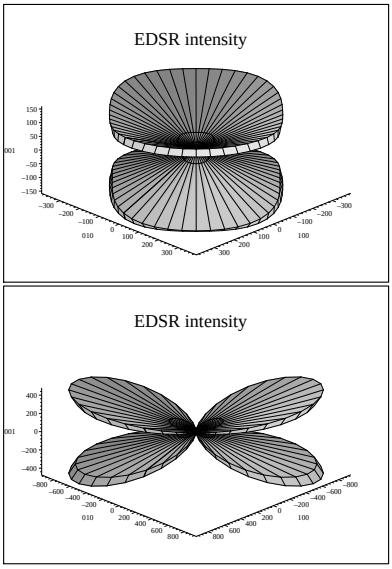

FIG. 1: The angular dependence of EDSR intensity $I(\theta,\varphi)$ (arb.units) for a [001] InSb quantum well with strain tensors $\epsilon_{xy}=0$ (top panel) and $\epsilon_{xy}=0.13\%$ (bottom panel). The other parameters are taken as $\omega_c/\omega_0=0.5$, $\omega_z/\omega_0=-0.16$, $\beta=1$, $\phi=\pi/4$, an imaginary part $i\delta(\delta=0.05\omega_0)$ was added to ω_c to eliminate the divergent pole.

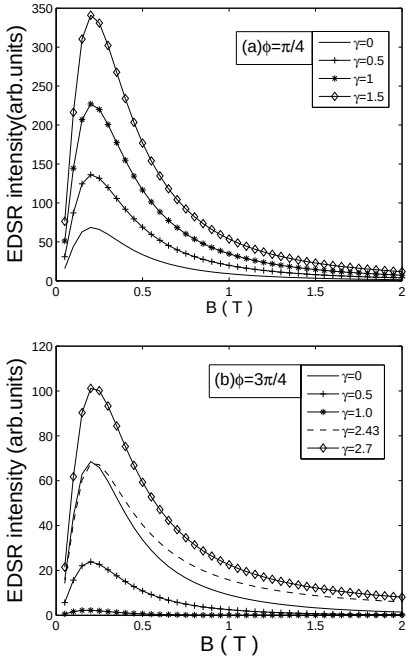

FIG. 2: The EDSR intensities versus the magnetic field in D+R case for two different external electric field along the directions (a) $\phi=\pi/4$ and (b) $\phi=3\pi/4$ with different strain strengths. Other parameters are taken as $m^\star=0.014m_0$, $\theta=0$, $\varphi=0$, $\delta=0.05\omega_0$ and $\beta=1$.

intensity change significantly. The supremum of the intensity will increase from 100 units to over 400 units after the shear strain $\epsilon_{xy}=\epsilon_0=0.13\%$, $\epsilon_0=2\beta/C_3$ is exerted. Additionally, the fourfold symmetry is broken down to a twofold symmetry.

Furthermore, we analyze the strain-induced effects in the spin manipulation in different situations. The magnetic field perpendicular to x-y plane of the quantum well, saying $\theta=0$ and $\varphi=0$, is introduced so that our conclusions can be verified by experiments conveniently. The dependence of the EDSR intensity on the direction of the ac electric field is plotted in the appendix, Fig. 5 (a), which shows a sinusoid-like behavior with amplitude and central value being determined by the strain strength. In Fig. 2, we plot the EDSR intensity versus the magnetic field for the ac electric field either along $\phi=\pi/4$ or $\phi=3\pi/4$ directions. Here, the unit of the EDSR intensity is $1/\hbar^2\omega_0^2$ with ω_0 being the same value as in Fig. 1; the other parameters are chosen as $\beta=1$, $\gamma_0=C_3\epsilon_0/2=1$, and $\epsilon_{xy}=\gamma\times\epsilon_0$. As shown in Fig. 2, the EDSR intensities reach an extreme value at a particular point B_R near $0.2T$ for both cases of $\phi=\pi/4$ and $\phi=3\pi/4$. If the confinement frequency ω_0 increases, the magnitude B_R at which the resonance occurs will increase simultaneously. Additionally, the location of the resonance peaks will undergo a slight change if the spin resonance frequency ω_z differs. Actually, the strain will affect g tensor which is relevant to ω_z. Thus the strain will bring in a shift in B_R, which is expected to be observed in experiments.

The peak value of EDSR intensity increases from 70 units to about 350 units as the strain strength increases from $\epsilon_{xy}=0$ to $\epsilon_{xy}=0.195\%$ when $\phi=\pi/4$. Four distinct curves are plotted in Fig 2(a), respectively. However, the variation trends change when the direction of ac electric field is changed from $\phi=\pi/4$ to $\phi=3\pi/4$ (see Fig. 2(b)). The peak value of the EDSR intensity is 70 units in the strain-free (*i.e.*, $\gamma=0$) case and decreases if the strain increases. It diminishes to zero when $\epsilon_{xy}=0.156\%$ (*i.e.*, $\gamma=1.2$), turns to increase after the strain strength exceeds $\epsilon_{xy}=0.156\%$ and reaches 70 units again when $\gamma=2.43$. From Fig. 2(b) together with Fig. 2(a), one can see that the strain-induced Rashba-type spin-orbit coupling combined with intrinsic Dresselhaus-type coupling can be verified by comparing two cases for the ac electric field along $\phi=\pi/4$ and $\phi=3\pi/4$ directions.

Let us make a qualitative analysis with respective to the above numerical calculations. The contribution of the first term in Eq. (11) is relatively small in comparison to the other terms when the well width is small and/or the temperature is sufficiently low, thus it can be neglected for a qualitative estimation. Then diagonal element of spin-flip transition matrix Eq. (11) dominates

$$\begin{aligned} T^{\mathrm{D}+R}\propto\quad & -\Omega[(\beta\sin\phi+\gamma\cos\phi)\\ & -i(\beta\cos\phi+\gamma\sin\phi)]. \end{aligned}$$

Consequently, the EDSR intensity behaves as

$$I^{\mathrm{D}+R}(\phi)\propto\Omega^2(\gamma^2+2\gamma\beta\sin 2\phi+\beta^2), \qquad (12)$$

From this equation, one can see that the EDSR intensity increases monotonously when $\phi = \pi/4$ while it firstly decreases and then increases when $\phi = 3\pi/4$ as the strain strength increases.

We also calculated the EDSR intensity when the magnetic field is tiled ($\theta \neq 0$). The corresponding results are similar to that for $\theta = 0$. Therefore electron spins can be sufficiently manipulated by using an *ac* electric field for the inversion asymmetry semiconductor quantum wells exerted with an appropriate strain.

The theoretical result in the above is expected to be measured experimentally. For this purpose, one may consider such a geometry that the InSb quantum well suffers from compression along the [110] axis. The electric field $\mathbf{E}(t)$ is in the plane of the 2DEG, and the magnetic field is perpendicular to the plane. A permanent uniaxial stress can be applied to the sample either with the help of a screw putting in the sample holder or by means of the other mechanical methods [15]. In the former approach, the strength of the uniaxial stress to the sample can be varied by adjusting the screw before structural failure occurs. One can measure the EDSR intensities for the *ac* electric field along $\phi = \pi/4$ ([110]) and $3\pi/4$ ([−110]) directions under certain strain strength. The measurement of EDSR intensity by tuning the strength of the uniaxial stress can accomplish the verification of theoretical results. The other approach is due to the fact that strain on samples can be realized in terms of a technique in growing by molecular beam epitaxy. A collection of those samples satisfying above strain configuration with different strain parameters are thus applicable for the same purpose.

B. Strain-induced Dresselhaus-type coupling

As a comparison, we consider other kind of semiconductor quantum wells. If the spin splitting induced by strain is assumed to be Dresselhuas-type, saying $H_{st}^{\rm D}$, while $H_{in}^{\rm D}$ is still dominant over $H_{in}^{\rm R}$ in these quantum wells, the total Hamiltonian describing the spin precession for electrons in such quantum wells (call D+D case for brevity) is written as

$$\begin{aligned} H_{so}^{\rm D+D} &= H_{in}^{\rm D} + H_{st}^{\rm D} \\ &= \sigma_x k_x(\lambda k_y^2 - \beta) + \sigma_y k_y(\beta - \lambda k_x^2) \\ &\quad +\gamma_1(\sigma_x k_x - \sigma_y k_y), \end{aligned} \tag{13}$$

with the strain configuration $\epsilon_{xx} = \epsilon_{yy}$ and $\gamma_1 = D(\epsilon_{zz} - \epsilon_{xx}) > 0$. The parameters λ, β and γ_1 are different for different kind of quantum wells. In the following part of this paper, we do not consider concrete materials in numerical calculation. In the lowest energy level $n_+ = n_- = 0$, the diagonal element of the spin-flip transition matrix $T^{\rm D+D}$ for $H_{so}^{\rm D+D}$ is calculated by using the similar method we employed in previous subsection,

$$\begin{aligned} T^{\rm D+D} &= -\frac{\lambda}{\hbar Q_3}\sum_{\nu=+,-}\Big\{\big[\omega_c\cos(\varphi-\phi)\cos\theta + i\omega_z\sin(\varphi-\phi)\big]\Omega Q_\nu Q_1 \\ &\quad +\big[\Omega\omega_c\cos\theta\sin(\varphi-\phi) - i\omega_z\cos(\varphi-\phi)(\Omega+\omega_c^2\sin^2\theta)\big]Q_\nu Q_2\Big\} + \frac{(\beta-\gamma_1)}{\hbar Q_3}\Big\{ \\ &\quad \cos(\varphi-\phi)\big[\Omega\omega_c\cos\theta(i\cos 2\varphi - \sin 2\varphi\cos\theta) + \omega_z(\Omega+\omega_c^2\sin^2\theta)(\sin 2\varphi - i\cos 2\varphi\cos\theta)\big] \\ &\quad +i\sin(\varphi-\phi)\Omega\big[\omega_z(i\cos 2\varphi - \sin 2\varphi\cos\theta) + \omega_c\cos\theta(\sin 2\varphi - i\cos 2\varphi\cos\theta)\big]\Big\}. \end{aligned} \tag{14}$$

We plot the EDSR intensity versus the magnetic field in the unit of $B_0 = \omega_0 m^\star c/2e$ for the D+D case in Fig. 3. We have chosen $\omega_z/\omega_c = -0.32$ and set $\beta = 1$, $\gamma_{10} = \beta$, and $\epsilon_{zz} - \epsilon_{xx} = \gamma_1 \times \gamma_{10}/D$ for convenience. Although the ratio ω_z/ω_c may differ for different quantum wells, the feature of the curves in Fig. 3 can manifest the main characteristics of the EDSR intensity for this kind of spin-orbit coupling. Since the concrete material is not specified here, we can only investigate the variation trends of the EDSR intensity with different strain strengths, which is adequate for the comparison between different combinations of spin-orbit couplings. As the strain strength increases, seen from Fig. 3, the EDSR intensities decrease at first; after the strain strength exceeds certain value it turns to increase in both cases $\phi = \pi/4$ and $\phi = 3\pi/4$. Actually, the EDSR intensity is independent of the direction of the *ac* electric field (see Fig. 5(b)). The distinct features in Fig. 2 and Fig. 3 are therefore suggested to identify whether the strain-induced spin splitting in a quantum well is Dresselhuas-type or Rashba-type by measuring the EDSR intensity in experiments.

IV. SYSTEMS WITH INTRINSIC RASHBA COUPLING

In this section, we consider the characteristics of EDSR for quantum wells with intrinsic Rashba-type spin split-

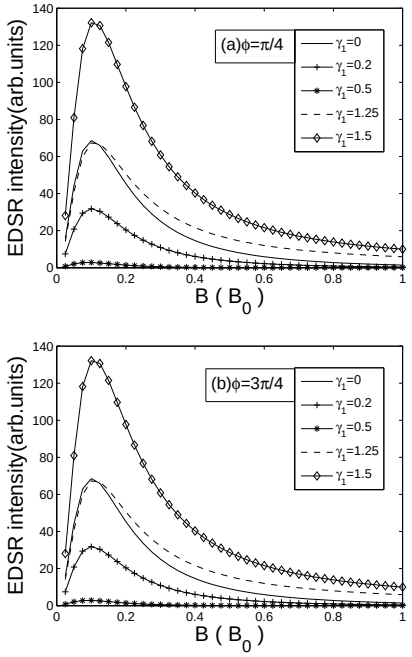

FIG. 3: The EDSR intensities versus the magnetic field in D+D case are plotted for (a) $\phi = \pi/4$ and (b) $\phi = 3\pi/4$. Here $B_0 = \omega_0 m^\star c/2e$ and the other parameters are taken as $\theta = 0$, $\varphi = 0$, $\delta = 0.05\omega_0$, $\beta = 1$, $\gamma_{10} = \beta$ and $\omega_z/\omega_c = -0.32$.

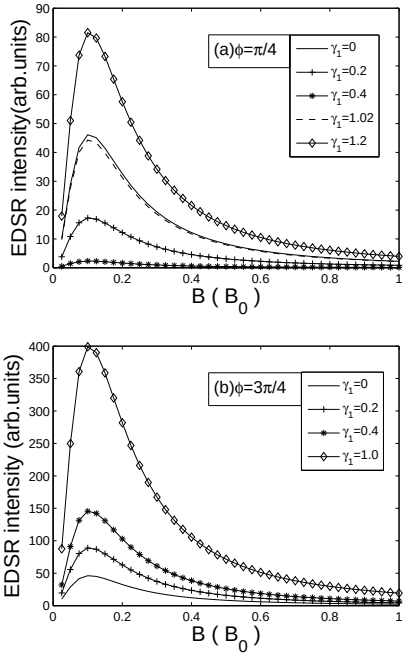

FIG. 4: The EDSR intensities versus the magnetic field in R+D case are plotted for (a) $\phi = \pi/4$ and (b) $\phi = 3\pi/4$. Here $B_0 = \omega_0 m^\star c/2e$ and the other parameters are taken as $\theta = 0$, $\varphi = 0$, $\delta = 0.05\omega_0$, $\alpha = 1$, $\gamma'_{10} = \alpha$ and $\omega_z/\omega_c = -0.32$.

ting due to structure inversion asymmetry, which is described by the Hamiltonian $H^{\rm R}_{in}$. Since the strain can introduce spin splittings of either Rashba-type $H^{\rm R}_{st}$ or Dresselhaus-type $H^{\rm D}_{st}$, the total Hamiltonian corresponding to R+R and R+D cases are, respectively,

$$\begin{aligned} H^{\rm R+R}_{so} &= \alpha(\sigma_x k_y - \sigma_y k_x) + \gamma(\sigma_x k_y - \sigma_y k_x), \\ H^{\rm R+D}_{so} &= \alpha(\sigma_x k_y - \sigma_y k_x) + \gamma_1(\sigma_x k_x - \sigma_y k_y). \end{aligned} \quad (15)$$

Here the definitions of parameters α, γ and γ_1 are the same as in the above, while their magnitudes depend on concrete materials and strain configurations. The Hamiltonians in Eqs. (15) describe systems with Rashba-type and Dresselhaus-type strain-induced spin splittings, respectively. Their corresponding diagonal elements of spin-flip transition matrices $T^{\rm R+R}$ and $T^{\rm R+D}$ are respectively obtained,

$$\begin{aligned} T^{\rm R+R} &= -\frac{(\gamma+\alpha)}{\hbar Q_3}\Big\{\cos(\varphi-\phi)\times \\ &\quad \big[\Omega\omega_c\cos^2\theta + \omega_z(\Omega+\omega_c^2\sin^2\theta)\big] \\ &\quad + i\cos\theta\sin(\varphi-\phi)(\omega_c+\omega_z)\Omega\Big\}, \end{aligned} \quad (16)$$

$$\begin{aligned} T^{\rm R+D} &= \frac{-\gamma_1}{\hbar Q_3}\Big\{\cos(\varphi-\phi)\times \\ &\quad \big[\Omega\omega_c\cos\theta(i\cos 2\varphi - \sin 2\varphi\cos\theta) \\ &\quad + \omega_z(\Omega+\omega_c^2\sin^2\theta)(\sin 2\varphi - i\cos 2\varphi\cos\theta)\big] \\ &\quad + i\sin(\varphi-\phi)\Omega\big[\omega_z(i\cos 2\varphi - \sin 2\varphi\cos\theta) \\ &\quad + \omega_c\cos\theta(\sin 2\varphi - i\cos 2\varphi\cos\theta)\big]\Big\} \\ &\quad - \frac{\alpha}{\hbar Q_3}\Big\{\cos(\varphi-\phi)\big[\Omega\omega_c\cos^2\theta + \omega_z(\Omega+\omega_c^2\sin^2\theta)\big] \\ &\quad + i\cos\theta\sin(\varphi-\phi)(\omega_c+\omega_z)\Omega\Big\}. \end{aligned} \quad (17)$$

For the R+R case, one can see from Eq. (16) that the EDSR intensity increases monotonously as the strain strength increases since $T^{\rm R+R} \propto (\gamma+\alpha)$ for either $\phi = \pi/4$ or $\phi = 3\pi/4$. For R+D case, using $T^{\rm R+D}$ in Eq. (17), we plot the EDSR intensity versus the magnetic field in the unit of $B_0 = \omega_0 m^\star c/2e$ in Fig. 4. The parameter choices of the plot are $\omega_z/\omega_c = -0.32$, $\theta = 0$, $\varphi = 0$, $\delta = 0.05\omega_0$, $\alpha = 1$, $\gamma'_{10} = \alpha$ and $\epsilon_{zz} - \epsilon_{xx} = \gamma_1 \times \gamma'_{10}/D$. Clearly, the intensity firstly decreases to zero and then increases after the strain strength exceeds $\gamma_1 = 0.5$ for $\phi = \pi/4$ (see Fig. 4(a)), which differs from the case in Fig. 2(a). As seen from Fig. 4(b) that the intensity increases monotonously along with the increment of strain strength when $\phi = 3\pi/4$, which is also different from the case in Fig. 2(b). The aforementioned features are consistent with Figs. 5(c) and 5(d) where the dependences of EDSR intensity on the direction of *ac* electric field are

illustrated for R+R and R+D cases, respectively.

V. CONCLUSION

We have analyzed the strain-assisted manipulation of electron spins in quantum wells where an *ac* electric field in x-y plane and a perpendicular magnetic field are applied. The strain effects on the manipulation are different for different semiconductor quantum wells. We exhibited that the efficiency of electron-spin manipulation can be enhanced by tuning the strain strength of the sample. There are four compositions for intrinsic and strain-induced spin splittings, namely, D+R, D+D, R+R, or R+D. These four situations can be distinguished from each other by changing the direction of the *ac* electric field from $\phi = \pi/4$ to $\phi = 3\pi/4$ and tuning the strain strengths in EDSR experiments. The effect combining those four kinds of spin splittings is helpful for understanding the experimental phenomena brought in by strain in some semiconductor quantum wells.

The work was supported by Program for Changjiang Scholars and Innovative Research Team in University, and by NSFC grant Nos. 10225419 and 10674117.

APPENDIX A

The dependence of EDSR intensities on the direction of the applied electric field are plotted for various strain strengths:

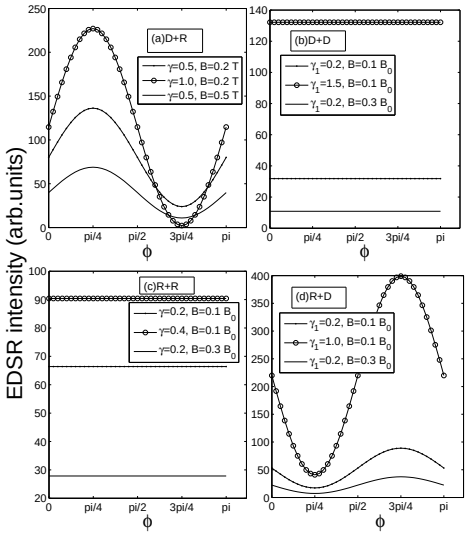

FIG. 5: The EDSR intensities versus ϕ, the direction of the *ac* electric field, with parameters $\omega_z/\omega_c = -0.32$, $\theta = 0$ and $\varphi = 0$ for the four cases: (a) D+R case, $\beta = 1$, $\epsilon_{xy} = \gamma \times \epsilon_0$, $\epsilon_0 = 2\beta/C_3 = 0.13\%$, $\omega_0 = 2eB_0/(m^\star c)$ with $B_0 = 2\,\mathrm{T}$. (b) D+D case, $\omega_0 = 2eB_0/(m^\star c)$, $\epsilon_{zz} - \epsilon_{xx} = \gamma_1 \times \gamma_{10}/D$, $\beta = 1$ and $\gamma_{10} = \beta$; (c) R+R case, $\omega_0 = 2eB_0/(m^\star c)$, $\epsilon_{xy} = \gamma \times \epsilon_0'$, $\epsilon_0' = 2\alpha/C_3$ and $\alpha = 1$; (d) R+D case, $\omega_0 = 2eB_0/(m^\star c)$, $\epsilon_{zz} - \epsilon_{xx} = \gamma_1 \times \gamma_{10}'/D$, $\alpha = 1$ and $\gamma_{10}' = \alpha$.

[1] S. A. Wolf, D. D. Awswchalom, R. A. Buhrma M. Daughton, S. Von. Molnar, M. L. Roukes, A Chtchelkanova, and D. M. Tresger, Science **294**, (2001).
[2] S. Datta and B. Das, Appl. Phys. Lett. **56**, 665 (19
[3] J. Schliemann, J. C. Egues, and D. Loss, Phys. Rev. **90**, 146801 (2003).
[4] I. Zutic, J. Fabian, and S. DasSarma, Rev. Mod. **76**, 323 (2004).
[5] D. Loss and D. P. DiVincenzo, Rev. Rev. A **57** (1998).
[6] Y. K. Kato, R. C. Myers, D. C. Driscoll, A. C. Gos J. Levy, and D. D. Awschalom, Science **299**, 1201 (2
[7] E. I. Rashba and Al. L. Efros, Phys. Rev. Lett 126405 (2003); Appl. Phys. Lett. **83**, 5295 (2003).
[8] Al. L. Efros and E. I. Rashba, Phys. Rev. B **73**, 1((2006).
[9] Y. K. Kato, R. C. Myers, A. C. Gossard, and I Awschalom, Nature (London) **427**, 50 (2004); Phys. Lett. **93**, 176601 (2004).
[10] S. A. Crooker and D. L. Smith, Phys. Rev. Lett. **94**, 236601 (2005).
[11] M. Beck, C. Metzner, S. Malzer, and G. H. Döhler, Europhys. Lett. **75**, 597 (2006).
[12] L. Jiang and M. W. Wu, Phys. Rev. B **72**, 033311(2005).
[13] M. Hruška, Š. Kos, S. A. Crooker, A. Saxena, and D. L. Smith, Phys. Rev. B **73**, 075306 (2006).
[14] H. Knotz, A. W. Holleitner, J. Stephens, R. C. Myers, and D. D. Awschalom, Appl. Phys. Lett. **88**, 241918 (2006).
[15] V. Sih, H. Knotz, J. Stephens, V. R. Horowitz, A. C. Gossard, and D. D. Awschalom, Phys. Rev. B**73**, 241316(R) (2006).
[16] B. A. Bernevig and S. C. Zhang, Phys. Rev. B **72**, 115204 (2005).
[17] M. I. D'yakonov and V. Yu. Kachorovskii, Fiz. Techn. Poluprov. **20**, 178 (1986)[Sov. Phys. Semicond. **20**, 110 (1986)].
[18] E. I. Rashba, Fiz. Tverd. Tela(Leningrad) **2**, 1224 (1960) [Sov. Phys. Solid State **2**, 1109 (1960)].
[19] Yu. A. Bychkov and E. I. Rashba, Pis'ma Zh. Eksp. Teor. Fiz. **39**, 66 (1984) [JETP Lett. **39**, 78 (1984)].
[20] F. Meier and B. P. Zakharchenya, Optical Orientation (North-Holland, Amsterdam 1984)
[21] W. K. Liu, X. M. Zhang, W. L. Ma, J. Winesett and M. B. Santos, J. Vac. Sci. Technol. B **14**, 2339 (1996).
[22] V. I. Perel', S. A. Tarasenko and I. N. Yassievich, *et al.*, Phys. Rev. B **67**, 201304(R) (2003).
[23] D. G. Seiler, B. D. Bajaj, and A. E. Stephens, Phys. Rev. B **16**, 2822 (1977).
[24] B. A. Bernevig and S. C. Zhang, Phys. Rev. Lett. **96**, 106802 (2006).
[25] R. Ranvaud, H. R. Trebin, U. Rössler and F. H. Pollak, Phys. Rev. B **20**, 701 (1979).